A sensation for inflation: initial swim bladder inflation in larval zebrafish is mediated by the mechanosensory lateral line.

Alexandra Venuto[1], Stacey Thibodeau-Beganny[2], Josef G. Trapani[2], Timothy Erickson[3]

1. Department of Biology, East Carolina University, Greenville, NC, USA.
2. Department of Biology and Neuroscience Program, Amherst College, Amherst, MA, USA.
3. Department of Biology, University of New Brunswick, Fredericton, NB, Canada.

Abstract

Larval zebrafish achieve neutral buoyancy by swimming up to the surface and taking in air through their mouths to inflate their swim bladders. We define this behavior as 'surfacing'. Little is known about the sensory basis for this underappreciated behavior of larval fish. A strong candidate is the mechanosensory lateral line, a hair cell-based sensory system that detects hydrodynamic information from sources like water currents, predators, prey, and surface waves. However, a role for the lateral line in mediating initial inflation of the swim bladder has not been reported.

To explore the connection between the lateral line and surfacing, we utilized a genetic mutant (*lhfpl5b*$^{-/-}$) that renders the zebrafish lateral line insensitive to mechanical stimuli. We observe that approximately half of these lateral line mutants over-inflate their swim bladders during initial inflation and become positively buoyant. Thus, we hypothesize that larval zebrafish use their lateral line to moderate interactions with the air-water interface during surfacing to regulate swim bladder inflation. To test the hypothesis that lateral line defects are responsible for swim bladder over-inflation, we show exogenous air is required for the hyperinflation phenotype and transgenic rescue of hair cell function restores normal inflation. We also find that chemical ablation of anterior lateral line hair cells in wild type larvae causes hyperinflation. Furthermore, we show that manipulation of lateral line sensory information results in abnormal inflation. Finally, we report spatial and temporal differences in the surfacing behavior between wild type and lateral line mutant larvae. In summary, we propose a novel sensory basis for achieving neutral buoyancy where larval zebrafish use their lateral line to sense the air-water interface and regulate initial swim bladder inflation.

Keywords: behavior, buoyancy, hair cells, hydrodynamics, lateral line, lhfpl5, swim bladder, sensory system, zebrafish

Introduction

The swim bladder of teleost fish provides for neutral buoyancy in the water column, thereby minimizing the energy expenditure associated with locomotion (Alexander, 1966). Larval teleosts initate swim bladder inflation by swimming up to the surface to ingest air using a set of behaviors we refer to as "surfacing" (Evans and Damant, 1928; Lindsey et al., 2010; von Ledebur, 1928). Although surfacing poses a significant risk of predation, larval fish are highly motivated to reach the surface to intake air. For example, pre-inflated lake trout larvae will swim hundreds of feet at a constant rate in attempts to access the surface (Tait, 1960). Surfacing is a complex task that requires a combination of newly developed physical features, sensory systems, and motor skills (Bailey and Doroshov, 1995; Chatain, 1989; Doroshev et al., 1981; Kimmel et al., 1995; Kitajima et al., 1994) – (i) Larvae must discriminate up from down and (ii) be able to move directionally towards the surface; (iii) they must appropriately sense the air-water interface, and (iv) be able to intake air through the mouth upon arrival at the surface. Ingested air is then moved by peristalsis into the swim bladder through the pneumatic duct that connects the gut and swim bladder (Doroshev et al., 1981; Rieger and Summerfelt, 1998; Tait, 1960). Together, surfacing represents perhaps the most complex behavior that larvae perform prior to achieving neutral buoyancy (Fero et al., 2011).

Little is known about the sensory cues that instruct the surfacing behavior. Perturbations to the vestibular system typically result in hypoinflation (Nicolson et al., 1998; Schoppik et al., 2017). The inability to detect gravity by the utricular otolith is specifically responsible for the phenotype, presumably because larvae are unable to orient their movements upwards towards the surface (Riley and Moorman, 2000). Photosensory cues may also play a role in directional orientation and surface detection. However, which photosensory systems are involved has not been defined and the effects of altering lighting conditions varies between species (Stuart and Drawbridge, 2012; Trotter et al., 2003; Villamizar et al., 2009). Even less is known about how larval fish detect the air-water interface itself. Fish and some amphibians possess an additional hair cell-based sensory system - the *mechanosensory lateral line* - that contributes to detection of near-field hydrodynamic information originating from water currents, predators and prey, conspecifics, abiotic objects, and surface waves (Anneser et al., 2020; Bleckmann, 2006; Butler and Maruska, 2016; Carrillo and McHenry, 2016; Mogdans, 2019; Montgomery et al., 1997; Stewart et al., 2013; Venuto et al., 2022). Specific to surface detection, surface-feeding fish use their lateral line to detect surface

62 waves created by their prey (Bleckmann and Schwartz, 1982). Furthermore, Japanese flying fish
63 are predicted to use their ventrally-located lateral line to sense transitions through the air-water
64 interface (Gibbs, 2004; Tsukamoto and Yoshino, 1957). While the lateral line is a strong candidate
65 to aid in surfacing behaviors that lead to initial swim bladder inflation in larval fish, its specific
66 role in this important behavior has not been explored.

67 A CRISPR-Cas9 knockout of *LHFPL tetraspan subfamily member 5b* (*lhfpl5b*) is the first
68 genetic zebrafish mutant where the lateral line is non-functional from birth but hearing and balance
69 are normal (Erickson et al., 2020). These mutants provide an opportunity to uncover novel roles
70 for the lateral line. Unexpectedly, homozygous mutant larvae present with a hyperinflation
71 phenotype characterized by over-filled swim bladders and positive buoyancy, a very rare finding
72 among swim bladder defects (Abbas and Whitfield, 2009; McCune and Carlson, 2004). Using
73 several genetic and chemical techniques to manipulate lateral line function, we show that lateral
74 line sensory information is used by larval zebrafish to appropriately fill their swim bladders, likely
75 by detecting surface tension at the air-water interface using mechanosensory neuromasts located
76 on their heads. Overall, our study uncovers a novel role for the mechanosensory lateral line
77 mediating initial inflation of the swim bladder.

78 **Methods**

79 *Animal husbandry and ethics statement*

80 Adult zebrafish (*Danio rerio*) were maintained and bred using standard procedures
81 (Westerfield, 2000). All experiments used larvae at 2-6 days post-fertilization (dpf), which are of
82 indeterminate sex at this stage. Except where otherwise stated, animals were placed in clear, plastic
83 tubs (dimensions: 15 cm x 10 cm x 4 cm, E3 volume: 460 mL) at 2 dpf and maintained at 28.5°C
84 on a 14:10 light/dark cycle at 500-700 lux in E3 embryo media (5 mM NaCl, 0.17 mM KCl, 0.33
85 mM CaCl2, 0.33 mM MgCl2, buffered with NaHCO3). Animal research complied with guidelines
86 stipulated by the Institutional Animal Care and Use Committees at East Carolina University
87 (protocol D372) and Amherst College (assurance number 3925-1 with the Office of Laboratory
88 Animal Welfare).

89 *Mutant and transgenic fish lines*

90 The zebrafish mutant allele *lhfpl5b*^{vo35} and transgenic lines *Tg(myo6b:EGFP-lhfpl5a)vo23*
91 and *Tg(myo6b:EGFP-PA)vo68* were used in this study (Erickson et al., 2017; Erickson et al.,

92 2020). For all experiments, *lhfpl5b*^{vo35} homozygotes were identified from their hetero- and
93 homozygous wild type siblings by lack of FM 1-43 (ThermoFisher) labeling of the lateral line hair
94 cells.

95 To create a fish line that expresses the Channelrhodopsin-2 (ChR2) optogenetic protein
96 solely in the hair cells of the lateral line, approximately 2 kb of DNA upstream of the start codon
97 of the *lhfpl5b* gene was cloned into the p5E plasmid of the recombination-based multisite Gateway
98 cloning system (ThermoFisher). A Tol2 transposon backbone was then used to create the injectable
99 expression plasmid *lhfpl5b2028:ChR2-EYFP-PA*. This plasmid was then co-injected with
100 transposase mRNA into single-cell embryos (Kwan et al., 2007) to create the
101 *Tg(lhfpl5b2028:ChR2-EYFP-PA)* zebrafish line.

102 *Buoyancy tests*

103 To ascertain the buoyancy status of larval fish, larvae were anesthetized with MS-222
104 (Western Chemical Inc., Ferndale, WA) and placed at the vertical midway point of a 50 mL conical
105 tube containing E3 media. At the expiration of a 30-second timer, the end position of the fish was
106 recorded and the fish was removed from the tube for imaging under the microscope. If the fish
107 reached the top or bottom of the tube before 30 seconds, then the time it took to reach that location
108 was recorded. The total height of the water column was 8.9 cm, and the fish was placed half-way
109 at 4.45 cm. The rate of buoyancy was determined by dividing the centimeters travelled by the
110 seconds it took to travel that distance (cm/s).

111 *Imaging and swim bladder measurements*

112 Swim bladders were imaged using a SteREO Discovery.V8 microscope (Zeiss) equipped
113 with a Gryphax Arktur camera (Jenoptik). Lateral and dorsal images of the swim bladder were
114 taken for each fish. Swim bladder measurements were conducted using the measurement tool in
115 Adobe Photoshop where measurements were calibrated according to the image of the stage
116 micrometer taken when imaging experiments. The major axis and minor axis of the lateral view of
117 the swim bladder was measured as well as the minor axis of the dorsal view. All measurements
118 were taken from numbered images so that the measurer was blinded to the genotype/condition.
119 These meaurements were halved and used in the equation for the volume of an ellipsoid: $V =$
120 $4/3\pi abc$ to find the volume of the swim bladder (Lindsey et al., 2010).
121

122 *Manipulation of photosensory cues during surfacing*

123 At 0 dpf, zebrafish embryos were collected and immediately placed in plastic tubs filled
124 with E3 (detailed above) in an unlit incubator. Larvae were not brought into light until 6 dpf, at
125 which point lateral line mutants and wild type siblings were identified by FM 1-43 labeling. After
126 sorting, larvae were analyzed for buoyancy. The experiment was repeated three times using 20-21
127 larvae (combined mutant and wild type) per trial.

128 *Blocking access to the air-water interface*

129 Mutant larvae and wild type siblings were sorted at 2 dpf into glass cylinders (diameter: 9.5
130 cm, E3 volume: 425 mL) equipped with fitted, wire mesh filter plungers (Bodum Inc., USA).
131 Conditions were as follows: wild type with open access to the surface, wild type with blocked
132 access to the surface, mutant with open access to the surface, and mutant with blocked access to
133 the surface. All containers were filled half way with E3 and in the experimental condition ("blocked
134 access"), the filter was pressed down below the surface for both wild type and mutant larvae. The
135 control condition used the same amount of E3 but the filter remained above the surface so that
136 larvae could access the exogenous air. Conditions remained constant until 6 dpf when larvae were
137 imaged and analyzed for swim bladder inflation. The experiment was repeated three times using
138 15-25 larvae per condition.

139 *Analysis of surfacing behavior*

140 Wild type and *lhfpl5b*^{vo35} larvae were blocked from having access to the surface until 9 AM
141 on 4 dpf when individuals were immediately placed into clear rectangular containers (dimensions:
142 3 cm x 3 cm x 3 cm, E3 volume: 20 mL) for video recording. Recordings lasted 12 hours, from 9
143 AM to 9 PM on 4 dpf. At the end of filming, larvae were imaged and analyzed for buoyancy and
144 swim bladder volume, as described. All surfacing videos were numbered for blind analysis.
145 Surfacing analysis was conducted by manual observation of each individual larvae from the videos
146 (30 frames per second) and manually counting visits made to the surface (counted as reaching the
147 meniscus), the timeframe of the video at which the surfacing event occurred, and the duration of
148 time spent at the surface per surfacing event. Recording was repeated six times with 3 mutant and
149 2 wild type larvae per recording. Larvae that did not inflate their swim bladders by the end of
150 filming were excluded from this analysis due to lack of surfacing events.
151

152 *Lateral line hair cell ablations*

153 For all experiments, wild type and *lhfpl5b* mutant larvae were treated with ototoxin with
154 untreated siblings acting as controls (n = 7-15 larvae per condition per trial, 4 trials) For single
155 treatments, surface accessed was blocked as described above for untreated and treated larvae until
156 9 AM on 4 dpf when treatment occurred. Single 30 minute treatments with neomycin sulfate (EMD
157 Millipore Corp., USA) were done with a 100 µm solution in E3 while repeated neomycin
158 treatments (Venuto and Erickson, 2021) were done as previously described with a concentration of
159 50 µM. For full ablation with copper sulfate (CuSO4; Ward's Science, Rochester, NY), the
160 treatment concentration was 10 uM with a 30 minute exposure. For experiments where head and
161 trunk neuromasts were selectively ablated, we anesthetized the larvae and pipetted them on agarose
162 gel. Excess water was removed and a thin layer of petroleum jelly (Vaseline, Unilever USA) was
163 placed horizontally at the back of the head. Next, 30 uM CuSO4 or E3 was pipetted onto the
164 appropriate region depending on the experimental condition. Immediately follow the 13 minute
165 treatment, larvae were placed in fresh E3 in clear tubs detailed above for 24 hours until 9 AM on 5
166 dpf when larvae were imaged and analyzed for swim bladder inflation. For all experiments, larvae
167 were imaged and analyzed for swim bladder inflation at 9 AM on 5 dpf. Each experiment was
168 repeated three times using 10-24 larvae per condition.

169 *Transgenic rescue of lateral line mutant*

170 Larval zebrafish from crosses of *lhfpl5b*$^{+/-}$ and *Tg(myo6b:EGFP-lhfpl5a)vo23Tg; lhfpl5b*$^{+/-}$
171 were sorted at 2 dpf for transgene expression. At 6 dpf, larvae were numbered, imaged for swim
172 bladder inflation and genotyped for the *lhfpl5b*^{vo35} allele as previously described (Erickson et al.,
173 2020). The experiment was repeated twice using 26-48 larvae per condition.

174 *Optogenetic activation of lateral line hair cells with Channelrhodopsin-2 (ChR2)*

175 After blocking access to the surface until 4 dpf, we exposed wild type and lateral line
176 mutants, with or without the *lhfpl5b2028:ChR2-EYFP-PA* transgene, to LED blue light (470 nm)
177 with an intensity of 730 lux over their holding tanks against a dark background. Light flashed for
178 25 milliseconds at one second intervals. Control larvae were kept in the same background, without
179 blue light exposure. Conditions were held constant until 6 dpf when larvae were imaged and
180 analyzed for swim bladder inflation. The experiment was repeated three times using 15-25 larvae
181 per condition.

182 *Oil-water interface experiments*

183 Mutant larvae and wild type siblings were sorted into clear cylindrical containers (diameter:
184 5 cm , volume: 60 mL) with embryo media only or embryo media with a 2 mm thick surface layer
185 of lab grade mineral oil (Ward's Science, Rochester, NY). Oil on the surface decreases surface
186 tension (Johansen, 1924) and has been previously used in experiments involving the zebrafish swim
187 bladder (Ehrlich and Schoppik, 2017). Conditions remained constant until 6 dpf when larvae were
188 imaged and analyzed for swim bladder volume. Because oil-filled larvae are negatively buoyant,
189 we did not perform buoyancy tests and classified larvae as over-filled based on swim bladder
190 volume alone. The experiment was repeated three times using 15-25 larvae per condition.

191 *Graphs and statistical tests*

192 All graphs and statistical tests were done using R (R Core Team, 2022). One-way ANOVAs
193 were used to compare the conditions as a whole (genotype independent variable plus environment
194 independent variable) with Tukey post-hoc test. Chi-squared tests were used to analyze proportion
195 data for over and under-inflation. For the over-inflation comparisons, the two categories used in
196 the comparison between conditions/genotypes were (i) over-inflation and (ii) all other inflation
197 (regular and under), meaning that totals per category/genotype accounted for 100% of the
198 population. Similarly, for the under-inflation comparisons, the two categories used in the
199 comparison between conditions/genotypes were (i) under-inflation and (ii) all other inflation
200 (regular and over). P-values less than 0.05 were considered significant.

201 **Results**

202 *Lateral line mutants exhibit a swim bladder hyperinflation phenotype*

203 The lateral line has not been previously implicated in initial inflation of the larval swim
204 bladder. As such, it was unexpected to observe that lateral line mutants (*lhfpl5b*$^{-/-}$) exhibit
205 hyperinflated swim bladders by 5-6 dpf (Figure 1A). We measured swim bladder volume and
206 buoyancy for each larva in the mutant and wild type populations (Figure 1B) and found that, on
207 average, 53.7% (SD = 6.4%, n = 41) of lateral line mutants over-inflate their swim bladders and
208 7.3% (SD = 7.1%, n = 41) under-inflate. For wild type larvae (including *lhfpl5b*^{vo35} heterozygotes),
209 0.0% (SD = 0.0%, n = 41) over-inflate and 4.9% (SD = 3.7%, n = 41) under-inflate their swim
210 bladders during initial inflation on average (Figure 1C). The proportion of over-inflation is
211 significantly different between mutant and wild type larvae (chi-square statistic: 70.45, $p <$
212 0.00001), while the proportion of under-inflation is not (chi-square statistic: 0.3546, p = 0.552).

213 Average swim bladder volume of mutant fish is larger (M = 0.012 mm^3, SD = 0.002 mm^3) than
214 wild type siblings (M = 0.0058 mm^3, SD = 0.00043 mm^3, $t(80) = 17.4$, $p < 0.0001$) (Figure 1D).
215 The proportions of neutrally and positively buoyant larvae do not change when raised in total
216 darkness (Supplemental Figure 1). This unexpected hyperinflation phenotype in *lhfpl5b*^{vo35}
217 homozygotes led us to investigate if the lateral line is contributing important sensory information
218 during the surfacing behavior.

219 *Access to the air-water interface is required for the hyperinflation phenotype of lateral line mutants*

220 For most teleosts, initial swim bladder inflation requires an intake of exogenous air,
221 typically from the water's surface. To test if the hyperinflation phenotype of lateral line mutants
222 requires access to surface air, we physically blocked access to the surface from 2-6 dpf (Figure 2).
223 On average, 0% (SD = 0.0%, n = 43) of blocked *lhfpl5b* mutants over-inflate their swim bladders,
224 which is significantly different from mutants with access to the surface (chi-square statistic: 70.45,
225 $p < 0.00001$; Figure 2B). The average swim bladder volume of blocked mutants (M = 0.0033 mm^3,
226 SD = 0.0015 mm^3) is significantly smaller than mutants with open access (M = 0.014 mm^3, SD =
227 0.0027 mm^3) (One-way ANOVA with Tukey post-test, $p < 0.00001$). Blocked mutant larvae had
228 statistically similar swim bladder volumes to blocked wild type larvae (M = 0.0037 mm^3, SD =
229 0.001 mm^3) (One-way ANOVA with Tukey post-test, $p = 0.927$) (Figure 2C). From these data, we
230 conclude that the *lhfpl5b* mutant hyperinflation phenotype requires intake of exogenous air and is
231 not caused by abnormal gas exchange from surrounding media nor excess internal gas production.

232 *Transgenic rescue of lateral line mutants restores normal inflation*

233 We next examined if lateral line defects are responsible for the hyper-inflation phenotype
234 of *lhfpl5b* mutants by restoring lateral line function in mutant larvae. We used the
235 *Tg(myo6b:EGFP-lhfpl5a)vo23* transgene, which uses a hair cell specific promoter (*myo6b*) to drive
236 a GFP-tagged *lhfpl5a* gene (Erickson et al., 2017). It has been shown that this *lhfpl5a* transgene
237 rescues lateral line hair cell function in *lhfpl5b*$^{-/-}$ *(or* lateral line) mutant fish (Erickson et al., 2020).
238 Using this rescue method, we observe no cases of hyperinflation in transgenic mutants (0%, SD =
239 0.0%, n = 17), which is significantly different from non-transgenic mutants (chi-square statistic:
240 82.12, $p < 0.00001$; Figure 3A). The average volume of the transgenic mutant swim bladder (M =
241 0.0057 mm^3, SD = 0.00001 mm^3) is significantly smaller than non-transgenic, *lhfpl5b* mutant
242 siblings (M = 0.0109 mm^3, SD = 0.0031 mm^3) (One-way ANOVA with Tukey post-test, p =
243 0.000003), but statistically similar to that of wild type transgenics (M = 0.0057 mm^3, SD = 0.0005

244 mm^3) (One-way ANOVA with Tukey post-test, $p = 0.979$, Figure 3B). Because the restoration of
245 *lhfpl5* function specifically in hair cells mitigates hyperinflation in *lhfpl5b* mutants, we conclude
246 that the phenotype is due to defects in sensory hair cell function and not caused by an unrecognized
247 role for *lhfpl5b* in another sensory organ or the swim bladder itself.

248 *Selective ablation of head neuromasts produces a hyperinflation phenotype in wild type larvae*

249 To further test if lateral line defects are responsible for the hyper-inflation phenotype seen
250 in *lhfpl5b* mutants, we ablated lateral line hair cells in wild type larvae using either neomycin
251 sulfate (neo) or copper sulfate (CuSO4) (Supplemental Figure 2 and Figure 4). Administering either
252 single or repeated neomycin treatments during the initial swim bladder inflation period of 3 - 4 dpf
253 results in a significant increase in the proportion of positively buoyant larvae (single neo chi-square
254 statistic: 9.95, $p = 0.0016$, repeated neo chi-square statistic: 34.88, $p < 0.0001$; Supplemental Figure
255 2A), but a non-significant increase in the average swim bladder volume (One-way ANOVA with
256 Tukey post-test, single neo $p = 1.0$, repeated neo p = 0.578; Supplemental Figure 2B). By
257 comparison, a single CuSO4 treatment results in a hyperinflation phenotype that is statistically
258 indistinguishable from lateral line mutants. An average of 59.6% ($SD = 7.7\%$, $n = 72$) of CuSO4-
259 treated wild types over inflate their swim bladders, which is significantly different from wild type
260 controls (chi-square statistic: 39.69, $p < 0.0001$; Supplemental Figure 2A). The average swim
261 bladder volume of the CuSO4-treated wild type larvae ($M = 0.0126$ mm^3, $SD = 0.0027$ mm^3) is
262 statistically similar to the average swim bladder volume of untreated lateral line mutants ($M =$
263 0.0139 mm^3, $SD = 0.0007$ mm^3) (One-way ANOVA with Tukey post-test, $p = 0.813$)
264 (Supplemental Figure 2B).

265 Since the anterior lateral line is likely to be the only part of the sensory organ to interact
266 with the air-water interface during surfacing, we predict that disruption of the head neuromasts will
267 result in hyperinflation and that trunk neuromasts will not play a role (Figure 4, Supplemental
268 Figure 3). Selective ablation of the anterior region with CuSO4 results in an average of 35.9% (SD
269 $= 10.1\%$, $n = 38$) hyperinflated larvae, which is significantly different from unablated controls (chi-
270 square statistic: 39.69, $p < 0.0001$; Figure 4B). Wild type larvae with head-specific ablations exhibit
271 a significant increase in average swim bladder volume ($M = 0.016$ mm^3, $SD = 0.0013$ mm^3)
272 compared to untreated wild type siblings ($M = 0.0012$ mm^3, $SD = 0.0013$ mm^3) (One-way ANOVA
273 with Tukey post-test, $p = 0.0365$) and statistically comparable swim bladder volumes to that of full
274 CuSO4-treated larvae ($M = 0.016$ mm^3, $SD = 0.0029$ mm^3) (One-way ANOVA with Tukey post-

275 test, p = 0.987) (Figure 4C). Conversely, tail-specific CuSO4 treatments do not cause
276 hyperinflation in wild type fish and result in statistically similar swim bladder volumes to untreated
277 siblings (M = 0.012 mm^3, SD = 0.0031 mm^3) (One-way ANOVA with Tukey post-test, p = 0.835)
278 (Figure 4C). The *lhfpl5b* mutant hyperinflation phenotype was not affected by either neomycin or
279 CuSO4 treatments (Supplemental Figure 2). Taken together, we conclude that the anterior region
280 of the lateral line system is critical to surface detection during initial swim bladder inflation.

281 *Decreasing surface tension results in over-filling of the swim bladder*

282 Surface tension is a characteristic that makes the air-water interface distinct from the rest
283 of the water column. We predict that larval fish sense this stimulus with their anterior lateral line
284 neuromasts and that by decreasing the interfacial tension, we would observe abnormal swim
285 bladder inflation in wild type larvae while lateral line mutants would be unaffected. The interfacial
286 tension between oil and water is approximately half that of air and water (Johansen, 1924). We
287 layered oil onto the surface of the embryo media and allowed larvae to perform surfacing behaviors
288 between 2-6 dpf (Figure 5). Using this experimental design, we find that the average swim bladder
289 volume of wild types exposed to an oil-water interface (M = 0.016 mm^3, SD = 0.0029 mm^3) is
290 significantly greater than the control group with access to an air-water interface (M = 0.007 mm^3,
291 SD = 0.001 mm^3) (One-way ANOVA with Tukey post-test, $p < 0.0001$). Furthermore, oil-exposed
292 wild types have statistically similar swim bladder volumes to that of *lhfpl5b* mutants (M = 0.014
293 mm^3, SD = 0.0038 mm^3) (One-way ANOVA with Tukey post-test, p = 0.886) (Figure 5C). Lateral
294 line mutants overfill their swim bladders to statistically similar proportions when presented with
295 either an air-water or oil-water interface (M = 0.01 mm^3, SD = 0.0026 mm^3) (One-way ANOVA
296 with Tukey post-test, p = 0.133). We conclude that surface tension is one of the surface
297 characteristics the lateral line is capable of detecting during initial swim bladder inflation.

298 *Optogenetic activation of lateral line hair cells prevents hyperinflation in lateral line mutant larvae*

299 If hydrodynamic information is informing the surfacing behaviors of larval fish, then
300 stimulus-independent manipulations of lateral line activity should alter their ability to correctly
301 inflate their swim bladders. To test this, we created the *Tg(lhfpl5b2028:ChR2-EYFP-PA)*
302 transgenic line that expresses the blue light activated channel, Channelrhodopsin-2, specifically in
303 lateral line hair cells (See Methods, Supplemental Figure 4). We predicted that optogenetic
304 stimulation of *lhfpl5b* mutants, whose lateral lines are insensitive to physical stimuli, would reduce
305 the frequency of the hyperinflation phenotype. Consistent with these predictions, under blue-light

306 stimulation, lateral line mutants with the *lhfpl5b:ChR2* transgene do not exhibit positive buoyancy
307 and have a significant decrease in average swim bladder volume (M = 0.0046 mm^3, SD = 0.0034
308 mm^3) compared to unstimulated transgenic mutants (M = 0.012 mm^3, SD = 0.0031 mm^3) (One-
309 way ANOVA with Tukey post-test, p = 0.00127) (Figure 6B). Transgenic wild types under blue
310 light exhibit a non-significant decrease in swim bladder volume (M = 0.0052 mm^3, SD = 0.004
311 mm^3) compared to unstimulated transgenic siblings (M = 0.0079 mm^3, SD = 0.002 mm^3) (One-way
312 ANOVA with Tukey post-test, p = 0.458). To demonstrate that blue light stimulation is reducing
313 swim bladder volumes via activation of lateral line hair cells, we treated wild type *lhfpl5b:ChR2*
314 larvae with CuSO4. As expected, we observe hyperinflation following CuSO4 treatment in
315 stimulated wild type *lhfpl5b:ChR2* larvae, with an average swim bladder volume (WT: M = 0.012
316 mm^3, SD = 0.0037 mm^3) that is statistically similar to experimental non-transgenic *lhfpl5b* mutants
317 (M = 0.011 mm^3, SD = 0.0024 mm^3) (One-way ANOVA with Tukey post-test, p = 0.998)
318 (Supplemental Figure 4B). Overall, optogenetic activation of mechanically-insensitive lateral line
319 organs in *lhfpl5b* mutants prevents the hyperinflation phenotype. Together, these data support the
320 hypothesis that the lateral line provides crucial sensory information during initial swim bladder
321 inflation in larval zebrafish.

322 *Lateral line mutants exhibit abnormal surfacing behaviors*

323 Our results suggest that larval fish are using their head neuromasts to sense the interfacial
324 tension between air and water at the surface. Even in wild type zebrafish, the interaction with the
325 surface during initial swim bladder inflation is not well characterized. To study this behavior in
326 more detail, we quantified the number of unique visits to the surface and the amount of time per
327 visit spent within the meniscus region from videos of wild type (n = 7) and mutant (n = 14) larvae
328 at 4 dpf. *lhfpl5b* mutants that will over-inflate their swim bladders make more visits (M = 87.3, SD
329 = 17.4) to the surface compared to both wild type (M = 42.0, SD = 16.3) and mutant siblings that
330 will inflate to normal proportions (M = 31.9, SD = 19.2) (One-way ANOVA with Tukey post-test,
331 p = 0.0004) (Figure 7A). Mutants destined for hyperinflation also spend more time (M = 139.0 s,
332 SD = 31.6 s) at the surface than normally-inflated wild type (M = 51.9 s, SD = 24.7 s) and mutant
333 siblings (M = 42.3 s, SD = 29.5 s) (One-way ANOVA with Tukey post-test, p = 0.00006) (Figure
334 7B). Since excess surfacing could be due to some mutants initiating the behavior earlier, we also
335 documented the time of the first surfacing event and found no significant difference between
336 neutrally buoyant and over-inflated larvae (Figure 7C). We conclude there is a correlation between

337 how larvae interact with the surface during the initial swim bladder inflation period and their
338 resulting swim bladder volume and buoyancy status.

339 **Discussion**

340 The intake of exogenous air from the surface is a common feature for intitial swim bladder
341 inflation in many species of fish (Furukawa et al., 2022; Goolish and Okutake, 1999; Jones and
342 Marshall, 1953; Korsøen et al., 2012; v. Ledebur and Wunder, 1937). However, few studies have
343 considered what sensory information is required to achieve neutral buoyancy. In this study, we
344 describe a new role for the mechanosensory lateral line in mediating initial inflation of the swim
345 bladder in zebrafish (Figure 8). Our data support a model in which larval zebrafish use their head
346 neuromasts to detect the air-water interface in support of their transition to neutral buoyancy.

347 *Lateral line defects in lhfpl5b mutants are responsible for hyperinflation phenotypes*

348 *lhfpl5b* mutant zebrafish are the first genetic model for the specific loss of lateral line
349 function in any organism (Erickson et al., 2020). These "lateral line mutants" exhibit an uncommon
350 swim bladder hyperinflation phenotype that prompted us to investigate this novel connection
351 between lateral line sensation and initial inflation of the swim bladder (Figure 1). Previous studies
352 have demonstrated that restricting access to surface air during the initial inflation period prevents
353 swim bladder inflation in larval zebrafish (Goolish and Okutake, 1999; Lindsey et al., 2011). In
354 addition, one study showed that some *solute carrier family 12 member 2* (*slc12a2 / nkcc1)* mutant
355 zebrafish over-fill their swim bladders and that blocking access to the surface prevents this
356 phenotype (Abbas and Whitfield, 2009), though further studies are required to determine the cause
357 of over-inflation in *slc12a2* mutants. Likewise, we find that blocking access to the air-water
358 interface eliminates over-inflation in lateral line mutants and greatly decreases average swim
359 bladder volumes of both mutant and wild type larvae (Figure 2). Our method of blocking access to
360 the air-water interface resulted in a small proportion of larvae (both wild type and mutant) inflating
361 their swim bladder to normal proportions, though hyperinflation was never observed. Inflation was
362 likely achieved by larvae accessing air bubbles that remain in the water after submerging the filter
363 (Goolish and Okutake, 1999). Overall, the hyperinflation phenotype in lateral line mutants requires
364 an intake of exogenous air, pointing to a sensory defect in *lhfpl5b* mutants rather than a
365 physiological one.

366 In support of this sensory-deficit hypothesis, we show the hyperinflation phenotype is
367 prevented by either transgenic rescue of *lhfpl5* function specifically in hair cells or optogenetic

368 stimulation of mechanically-insensitive lateral line hair cells in *lhfpl5b* mutants (Figures 3 and 6).
369 Furthermore, chemical ablation of lateral line hair cells in wild type larvae prior to initial inflation
370 can phenocopy the *lhfpl5b* mutant. A single treatment with CuSO4 caused similar swim bladder
371 over-inflation proportions to lateral line mutants (Supplemental Figure 2). Repeated neomycin
372 treatments over 3-4 dpf caused the next highest percentage of swim bladder over-inflation and a
373 single neomycin treatment only resulted in a few cases of wild type over-inflation. These results
374 agree with previous work showing rapid hair cell regeneration following neomycin treatment and
375 comparatively slower recovery after CuSO4 exposure (Hernández et al., 2006; Mackenzie and
376 Raible, 2012; Murakami et al., 2003; Santos et al., 2006; Venuto and Erickson, 2021). Thus, via
377 multiple genetic and chemical approaches, our data show that lateral line hair cell activity can
378 modulate swim bladder inflation in larval zebrafish.

379 Ototoxins have been extensively used to study lateral line-mediated behaviors in free-
380 swimming larvae and adult fish (Baker and Montgomery, 1999; Bleckmann, 2006; Coffin and
381 Ramcharitar, 2016; Montgomery et al., 1997; Pavlov and Tyuryukov, 1993). However, we are not
382 aware of any behavioral studies where the lateral line was disrupted prior to larvae achieving
383 neutral buoyancy, likely explaining why this connection between the lateral line and initial swim
384 bladder inflation has not been noted in current literature. Interestingly, an 1896 study predicted a
385 relationship between the lateral line and swim bladder inflation, since disruption of the lateral line
386 in adult goldfish resulted in "swelling of the swim bladder" and positive buoyancy (Richard, 1896).
387 However, it is not clear if the phenotypic similarities between these adult goldfish and our
388 experimental larval zebrafish share the same underlying causes. Regarding roles for the lateral line
389 in early life behaviors, a close parallel to our findings is the report that unhatched red-eyed treefrogs
390 use their lateral line organ to mediate mechanosensory-cued hatching (Jung et al., 2020). In this
391 case, the frog lateral line can sense vibrational stimuli, such as that produced by predators, and
392 promote escape hatching behaviors even before the onset of vestibular function. Similarly, our data
393 suggest that the lateral line is modulating early locomotor activities in zebrafish prior to the
394 development of fully formed vestibular or rheotactic responses (Bagnall and Schoppik, 2018; Mo
395 et al., 2010; Olive et al., 2016). As such, the involvement of lateral line in the surfacing behavior
396 may represent the earliest behavioral role for the lateral line yet described.

397 *Head neuromasts are required for normal swim bladder inflation, likely by sensing surface tension*

398 We expanded on the full-body lateral line ablation experiments with specific ablations of

399 either the head or truck neuromasts with CuSO4. Previous studies have shown that head neuromasts
400 are involved with detection of surface features and prey capture (Bleckmann, 1988; Carrillo and
401 McHenry, 2016; Müller and Schwartz, 1982; Schwartz and Hasler, 1966). Indeed, ablation of the
402 head neuromasts in wild type larvae recapitulated the hyperinflation phenotype of *lhfpl5b* mutants
403 while ablation of the tail neuromasts had no effect on either swim bladder volume or buoyancy
404 (Figure 4). These findings suggest that the head neuromasts interact with the air-water interface
405 during surfacing and that the posterior lateral line is dispensible for achieving neutral buoyancy.
406 As such, our findings also provide additional support for the anterior lateral line as a central
407 mediator of surface-related behaviors in fish.

408 The interfacial tension between air and water represents a unique hydrodynamic stimulus
409 that may be detected by the lateral line. The tension between oil and water is half that of air and
410 water (Johansen, 1924). Thus, by adding a layer of oil to the surface, we predicted that surface
411 detection would become increasingly difficult and result in over-filling of the swim bladder. We
412 find that, when given access to an oil-water interface, wild type larvae over-fill their swim bladders
413 with oil to a statistically similar volume as lateral line mutants who overinflate with air (Figure 6).
414 We interpret this result as support for the hypothesis that the lateral line senses interfacial tension
415 between air and water as larvae interact with the surface during initial swim bladder inflation. This
416 interpretation is further supported by the observation that *lhfpl5b* mutants (who are already
417 insensitive to interfacial tension) exhibit similar swim bladder volumes when exposed to either oil
418 or air. However, a possible complementary interpretation for these data is that larvae who fill their
419 swim bladders with oil may be deprived of the normal feedback on buoyancy levels as they intake
420 from the surface. Since oil is denser than air, oil-filled larvae are negatively buoyant. In this
421 scenario, larvae may continue to visit the surface for air intake in an attempt to achieve neutral
422 buoyancy. However, future studies are required to examine if such a feedback mechanism exists in
423 larval zebrafish.

424 *Swim bladder over-inflation is correlated with excess time spent at the air-water interface*

425 Since our data suggest that the air-water interface is providing a distinct stimulus to the
426 lateral line, we investigated whether surface interactions differed between hyperinflated *lhfpl5b*
427 mutants and their wild type counterparts. As predicted, over-inflated mutants took more visits *and*
428 spent more time at the surface than neutrally-buoyant mutant and wild type siblings (Figure 7).
429 Excess breaching of the surface occurred despite over-inflated and neutrally buoyant larvae

430 exhibiting similar timing for their first surfacing attempts. While it is unclear whether larvae ingest
431 air during the entirety of the duration spent above the air-water interface, it is known that surface
432 breaches are observed during initial inflation (Goolish and Okutake, 1999; Lindsey et al., 2010;
433 Rieger and Summerfelt, 1998). Therefore, the increase in surface visits likely leads to an increase
434 in air deposition to the swim bladder in lateral line mutants.

435 *Multisensory integration during the surfacing behavior*

436 Interestingly, approximately half of all lateral line mutants inflate their swim bladders to
437 normal proportions and continue to develop into viable adults. To account for this fact, we
438 hypothesize that additional somatosensory, photosensory, or mechanosensory systems may
439 compensate for the loss of lateral line sensation and help mutant larvae achieve neutral buoyancy
440 (Riley and Moorman, 2000; Suchocki and Sepulveda-Villet, 2019; Trotter et al., 2003). The lateral
441 line is involved several multi-sensory behaviors, including flow orientation (Bak-Coleman et al.,
442 2013; Coombs et al., 2020; Liao, 2006), prey capture (Carrillo and McHenry, 2016; Nelson et al.,
443 2002; New, 2002), and predator avoidance (Free et al., 2019; Jung et al., 2020; Stewart et al., 2013),
444 and we predict that surfacing can be added to this list.

445 The photosensory and mechanosensory systems exhibit distinct organizational patterns for
446 primary input to the central nervous system — even the anterior and posterior lateral line ganglia
447 primary projections are somatotopically organized in zebrafish larvae (Alexandre et al., 1999;
448 Fame et al., 2006; Hale et al., 2016; Liao and Haehnel, 2012; McCormick, 1989; Mirjany and
449 Faber, 2011). The Mauthner neurons integrate multisensory input at the level of the hindbrain, but
450 the surfacing behavior is unlikely to use this circuit. For higher order processing however,
451 information from the lateral line, vestibular, and photosensory systems are integrated in various
452 brain regions. The thalamus is one such sensory integration center in zebrafish (Mueller, 2012).
453 Socially-relevant mechanosensory and photosensory information is represented in a thalamic
454 region marked by the expression of *parathyroid hormone 2* (*pth2*) and *somatostatin 7* (*sst7*)
455 (Anneser et al., 2020; Kappel et al., 2022; Venuto et al., 2022). Vestibular information is also
456 represented in the thalamus (Favre-Bulle et al., 2018; Migault et al., 2018), though it is not clear if
457 the exact same region is involved. Photosensory, lateral line, and vestibular/auditory information
458 is also integrated in the tectum (Favre-Bulle et al., 2018; Filosa et al., 2016; Isa et al., 2021; Migault
459 et al., 2018). In fact, neurons in the periventricular layer (PVL) of the tectum, which is similar to
460 the superior colliculus in mammals, respond to visual, auditory, and lateral line inputs (Ingle, 1973;

King et al., 1996; Perrault et al., 2011; Thompson et al., 2016). However, it is hypothesized that most of these modalities are processed in parallel at younger stages of development (Thompson et al., 2016). It is worth noting that these sensory systems are in developing stages during surfacing behaviors.

Photosensory cues did not alter the buoyancy status of either wild type or *lhfpl5b* mutant larvae (Supplemental Figure 1), suggesting that, at most, photosensory systems play a subtle modulatory role in the surfacing behavior of larval zebrafish. The vestibular system is likely required to coordinate the vertical orientation and climbing portions of surfacing (Bagnall and Schoppik, 2018; Ehrlich and Schoppik, 2017; Ehrlich and Schoppik, 2019). Meanwhile, our data support the idea that the lateral line is responsible for the surface detection and breaching aspects of surfacing. However, given that both the vestibular and lateral line systems are providing spatial information in during the surfacing behavior, there may be crosstalk between them. For example, the vestibular system must quickly adapt to a dynamic increase in buoyancy over the course of multiple breaching events, so feedback from the lateral line during surface interactions may help fine tune the vestibular sense. However, the link between these systems have not been well-investigated during deliberate behaviors like surfacing (Chagnaud et al., 2017; Liu et al., 2021). So, while sensory integration exists in zebrafish and seems necessary for larvae to achieve neutral buoyancy, the integration dynamics are unclear during the intial swim bladder inflation timeframe and require future investigation.

Acknowledgements

The authors would like to thank Dr. Fadi Issa (ECU) for his support and technical advice. The authors also thank the Issa, Trapani, and Erickson lab members for fish care and maintenance.

Author contributions

Conceptualization: A.V., T.E.; Methodology: A.V., J.G.T., T.E.; Validation: A.V.; Formal analysis: A.V.; Investigation: A.V.; Resources: S.T-B., J.G.T; Writing - original draft: A.V., T.E.; Writing - review & editing: A.V., J.G.T., T.E..; Visualization: A.V.; Supervision: T.E.; Project administration: T.E.; Funding acquisition: J.G.T., T.E.

Funding

This work was supported by funding from East Carolina University's Division of Research, Economic Development and Engagement (REDE) and a Natural Science and Engineering

Research Council (NSERC) Discovery Grant (RGPIN-2021-03166) to T.E., a National Institute on Deafness and Other Communication Disorders (NIDCD) award to J.G.T. (NIH R15DC014843), and East Carolina Department of Biology funding provided to A.V..

References

Abbas, L. and Whitfield, T. T. (2009). Nkcc1 (Slc12a2) is required for the regulation of endolymph volume in the otic vesicle and swim bladder volume in the zebrafish larva. *Development* **136**, 2837–2848.

Alexander, R. M. (1966). Physical aspects of swimbladder function. *Biol Rev Camb Philos Soc* **41**, 141–176.

Alexandre, D., Ghysen, A. and Ghysen, A. (1999). Somatotopy of the lateral line projection in larval zebrafish. *Proc Natl Acad Sci U S A* **96**, 7558–62.

Anneser, L., Alcantara, I. C., Gemmer, A., Mirkes, K., Ryu, S. and Schuman, E. M. (2020). The neuropeptide Pth2 dynamically senses others via mechanosensation. *Nature* **588**, 653–657.

Bagnall, M. W. and Schoppik, D. (2018). Development of vestibular behaviors in zebrafish. *Curr Opin Neurobiol* **53**, 83–89.

Bailey, H. C. and Doroshov, S. I. (1995). The duration of the interval associated with successful inflation of the swimbladder in larval striped bass (Morone saxatilis). *Aquaculture* **131**, 135–143.

Bak-Coleman, J., Court, A., Paley, D. A. and Coombs, S. (2013). The spatiotemporal dynamics of rheotactic behavior depends on flow speed and available sensory information. *J Exp Biol* **216**, 4011–24.

Baker, C. F. and Montgomery, J. C. (1999). The sensory basis of rheotaxis in the blind Mexican cave fish, Astyanax fasciatus. *J Comp Physiol A* **184**, 519–527.

Bleckmann, H. (1988). Prey Identification and Prey Localization in Surface-feeding Fish and Fishing Spiders. In *Sensory Biology of Aquatic Animals*, pp. 619–641. New York, NY: Springer New York.

Bleckmann, H. (2006). The Lateral Line System of Fish. *Fish Physiology* **25**, 411–453.

Bleckmann, H. and Schwartz, E. (1982). The functional significance of frequency modulation within a wave train for prey localization in the surface-feeding fishAplocheilus lineatus (Cyprinodontidae). *Journal of Comparative Physiology A* **145**, 331–339.

Butler, J. M. and Maruska, K. P. (2016). Mechanosensory signaling as a potential mode of communication during social interactions in fishes. *J Exp Biol* **219**, 2781–2789.

Carrillo, A. and McHenry, M. J. (2016). Zebrafish learn to forage in the dark. *Journal of Experimental Biology* **219**, 582–589.

Chagnaud, B. P., Engelmann, J., Fritzsch, B., Glover, J. C. and Straka, H. (2017). Sensing External and Self-Motion with Hair Cells: A Comparison of the Lateral Line and Vestibular Systems from a Developmental and Evolutionary Perspective. *Brain Behav Evol* **90**, 98–116.

Chatain, B. (1989). Problems related to the lack of functional swimbladder in intensive rearing of Dicentrarchus labrax and Sparus auratus. *Advances in Tropical Aquaculture, Workshop at Tahiti, French Polynesia, 20 Feb - 4 Mar 1989*.

Coffin, A. B. and Ramcharitar, J. (2016). Chemical Ototoxicity of the Fish Inner Ear and Lateral Line BT - Fish Hearing and Bioacoustics: An Anthology in Honor of Arthur N.

535 Popper and Richard R. Fay. In (ed. Sisneros, J. A.), pp. 419–437. Cham: Springer
536 International Publishing.
537 **Coombs, S., Bak-Coleman, J. and Montgomery, J.** (2020). Rheotaxis revisited: a multi-
538 behavioral and multisensory perspective on how fish orient to flow. *Journal of Experimental*
539 *Biology* **223**,.
540 **Doroshev, S., Cornacchia, J. and Hogan, K.** (1981). Initial swim bladder inflation in the larvae
541 of physoclistous fishes and its importance for larval culture. *Rapports et Proces-verbaux des*
542 *Réunions Cons. int. Explor. Mer* **178**, 495–500.
543 **Ehrlich, D. E. and Schoppik, D.** (2017). Control of Movement Initiation Underlies the
544 Development of Balance. *Current Biology* **27**, 334–344.
545 **Ehrlich, D. E. and Schoppik, D.** (2019). A primal role for the vestibular sense in the
546 development of coordinated locomotion. *Elife* **8**,.
547 **Erickson, T., Morgan, C. P., Olt, J., Hardy, K., Busch-Nentwich, E., Maeda, R., Clemens,**
548 **R., Krey, J. F., Nechiporuk, A., Barr-Gillespie, P. G., et al.** (2017). Integration of Tmc1/2
549 into the mechanotransduction complex in zebrafish hair cells is regulated by
550 Transmembrane O-methyltransferase (Tomt). *Elife* **6**,.
551 **Erickson, T., Pacentine, I. V., Venuto, A., Clemens, R. and Nicolson, T.** (2020). The lhfpl5
552 Ohnologs lhfpl5a and lhfpl5b Are Required for Mechanotransduction in Distinct
553 Populations of Sensory Hair Cells in Zebrafish. *Front Mol Neurosci* **12**, 320.
554 **Evans, H. M. and Damant, G. C. C.** (1928). Observations on the Physiology of the Swim
555 Bladder in Cyprinoid Fishes. *Journal of Experimental Biology* **6**, 42–55.
556 **Fame, R. M., Brajon, C. and Ghysen, A.** (2006). Second-order projection from the posterior
557 lateral line in the early zebrafish brain. *Neural Dev* **1**, 4.
558 **Favre-Bulle, I. A., Vanwalleghem, G., Taylor, M. A., Rubinsztein-Dunlop, H. and Scott, E.**
559 **K.** (2018). Cellular-Resolution Imaging of Vestibular Processing across the Larval Zebrafish
560 Brain. *Current Biology* **28**, 3711-3722.e3.
561 **Fero, K., Yokogawa, T. and Burgess, H. A.** (2011). The behavioral repertoire of larval
562 zebrafish. *Neuromethods* **52**, 249–291.
563 **Filosa, A., Barker, A. J., Dal Maschio, M. and Baier, H.** (2016). Feeding State Modulates
564 Behavioral Choice and Processing of Prey Stimuli in the Zebrafish Tectum. *Neuron* **90**,
565 596–608.
566 **Free, B. A., McHenry, M. J. and Paley, D. A.** (2019). Probabilistic analytical modelling of
567 predator–prey interactions in fishes. *J R Soc Interface* **16**, 20180873.
568 **Furukawa, S., Machida, Y., Takeuchi, K., Hoshikawa, Y. and Irie, K.** (2022). Failure to gulp
569 surface air induces swim bladder adenomas in Japanese medaka (Oryzias latipes). *J Toxicol*
570 *Pathol* **35**, 237–246.
571 **Gibbs, M. A.** (2004). Lateral Line Receptors: Where Do They Come from Developmentally and
572 Where Is Our Research Going? *Brain Behav Evol* **64**, 163–181.
573 **Goolish, E. M. and Okutake, K.** (1999). Lack of gas bladder inflation by the larvae of zebrafish
574 in the absence of an air-water interface. *J Fish Biol* **55**, 1054–1063.
575 **Hale, M. E., Katz, H. R., Peek, M. Y. and Fremont, R. T.** (2016). Neural circuits that drive
576 startle behavior, with a focus on the Mauthner cells and spiral fiber neurons of fishes.
577 *https://doi-org.proxy.hil.unb.ca/10.1080/01677063.2016.1182526* **30**, 89–100.
578 **Hernández, P. P., Moreno, V., Olivari, F. A. and Allende, M. L.** (2006). Sub-lethal
579 concentrations of waterborne copper are toxic to lateral line neuromasts in zebrafish (Danio
580 rerio). *Hear Res* **213**, 1–10.

Ingle, D. (1973). Evolutionary perspectives on the function of the optic tectum. *Brain Behav Evol* **8**, 211–237.

Isa, T., Marquez-Legorreta, E., Grillner, S. and Scott, E. K. (2021). The tectum/superior colliculus as the vertebrate solution for spatial sensory integration and action. *Current Biology* **31**, R741–R762.

Johansen, E. M. (1924). The Interfacial Tension between Petroleum Products and Water. *Ind Eng Chem* **16**, 132–135.

Jones, F. R. H. and Marshall, N. B. (1953). The structure and functions of the teleostean swimbladder. *Biological Reviews* **28**, 16–82.

Jung, J., Serrano-Rojas, S. J. and Warkentin, K. M. (2020). Multimodal mechanosensing enables treefrog embryos to escape egg-predators. *J Exp Biol* **223**,.

Kappel, J. M., Förster, D., Slangewal, K., Shainer, I., Svara, F., Donovan, J. C., Sherman, S., Januszewski, M., Baier, H. and Larsch, J. (2022). Visual recognition of social signals by a tectothalamic neural circuit. *Nature 2022 608:7921* **608**, 146–152.

Kimmel, C. B., Ballard, W. W., Kimmel, S. R., Ullmann, B. and Schilling, T. F. (1995). Stages of embryonic development of the zebrafish. *Developmental Dynamics* **203**, 253–310.

King, A. J., Schnupp, J. W. H., Carlile, S., Smith, A. L. and Thompson, I. D. (1996). The development of topographically-aligned maps of visual and auditory space in the superior colliculus. *Prog Brain Res* **112**, 335–350.

Kitajima, C., Watanabe, T., Tsukashima, Y. and Fujita, S. (1994). Lordotic Deformation and Abnormal Development of Swim Bladders in Some Hatchery-Bred Marine Physoclistous Fish in Japan. *J World Aquac Soc* **25**, 64–77.

Korsøen, Ø. J., Fosseidengen, J. E., Kristiansen, T. S., Oppedal, F., Bui, S. and Dempster, T. (2012). Atlantic salmon (Salmo salar L.) in a submerged sea-cage adapt rapidly to re-fill their swim bladders in an underwater air filled dome. *Aquac Eng* **51**, 1–6.

Kwan, K. M., Fujimoto, E., Grabher, C., Mangum, B. D., Hardy, M. E., Campbell, D. S., Parant, J. M., Yost, H. J., Kanki, J. P. and Chien, C. bin (2007). The Tol2kit: a multisite gateway-based construction kit for Tol2 transposon transgenesis constructs. *Dev Dyn* **236**, 3088–3099.

Liao, J. C. (2006). The role of the lateral line and vision on body kinematics and hydrodynamic preference of rainbow trout in turbulent flow. *J Exp Biol* **209**, 4077–90.

Liao, J. C. and Haehnel, M. (2012). Physiology of afferent neurons in larval zebrafish provides a functional framework for lateral line somatotopy. *J Neurophysiol* **107**, 2615–2623.

Lindsey, B. W., Smith, F. M. and Croll, R. P. (2010). From inflation to flotation: Contribution of the swimbladder to whole-body density and swimming depth during development of the zebrafish (Danio rerio). *Zebrafish* **7**, 85–96.

Lindsey, B. W., Dumbarton, T. C., Moorman, S. J., Smith, F. M. and Croll, R. P. (2011). Effects of simulated microgravity on the development of the swimbladder and buoyancy control in larval zebrafish (Danio rerio). *J Exp Zool A Ecol Genet Physiol* **315A**, 302–313.

Liu, Z., Hildebrand, D. G. C., Morgan, J. L., Slimmon, N. and Bagnall, M. W. (2021). The organization of the gravity-sensing system in zebrafish. *bioRxiv* 2021.07.09.451839.

Mackenzie, S. M. and Raible, D. W. (2012). Proliferative Regeneration of Zebrafish Lateral Line Hair Cells after Different Ototoxic Insults. *PLoS One* **7**, 47257.

McCormick, C. A. (1989). Central Lateral Line Mechanosensory Pathways in Bony Fish. *The Mechanosensory Lateral Line* 341–364.

McCune, A. R. and Carlson, R. L. (2004). Twenty ways to lose your bladder: Common natural mutants in zebrafish and widespread convergence of swim bladder loss among teleost fishes. *Evol Dev* **6**, 246–259.

Migault, G., Plas, T. L. van der, Trentesaux, H., Panier, T., Candelier, R., Proville, R., Englitz, B., Debrégeas, G. and Bormuth, V. (2018). Whole-Brain Calcium Imaging during Physiological Vestibular Stimulation in Larval Zebrafish. *Current Biology* **28**, 3723-3735.e6.

Mirjany, M. and Faber, D. S. (2011). Characteristics of the anterior lateral line nerve input to the Mauthner cell. *Journal of Experimental Biology* **214**, 3368–3377.

Mo, W., Chen, F., Nechiporuk, A. and Nicolson, T. (2010). Quantification of vestibular-induced eye movements in zebrafish larvae. *BMC Neurosci* **11**, 110.

Mogdans, J. (2019). Sensory ecology of the fish lateral-line system: Morphological and physiological adaptations for the perception of hydrodynamic stimuli. *J Fish Biol* **95**, 53–72.

Montgomery, J. C., Baker, C. F. and Carton, A. G. (1997). The lateral line can mediate rheotaxis in fish. *Nature* **389**, 960–963.

Mueller, T. (2012). What is the thalamus in zebrafish? *Front Neurosci* **6**, 64.

Müller, U. and Schwartz, E. (1982). Influence of single neuromasts on prey localizing behavior of the surface feeding fish, Aplocheilus lineatus. *Journal of Comparative Physiology A* **149**, 399–408.

Murakami, S. L., Cunningham, L. L., Werner, L. A., Bauer, E., Pujol, R., Raible, D. W. and Rubel, E. W. (2003). Developmental differences in susceptibility to neomycin-induced hair cell death in the lateral line neuromasts of zebrafish (Danio rerio). *Hear Res* **186**, 47–56.

Nelson, M. E., MacIver, M. A. and Coombs, S. (2002). Modeling Electrosensory and Mechanosensory Images during the Predatory Behavior of Weakly Electric Fish. *Brain Behav Evol* **59**, 199–210.

New, J. G. (2002). Multimodal Integration in the Feeding Behaviors of Predatory Teleost Fishes. *Brain Behav Evol* **59**, 177–189.

Nicolson, T., Rüsch, A., Friedrich, R. W., Granato, M., Ruppersberg, J. P. and Nüsslein-Volhard, C. (1998). Genetic analysis of vertebrate sensory hair cell mechanosensation: The zebrafish circler mutants. *Neuron* **20**, 271–283.

Olive, R., Wolf, S., Dubreuil, A., Bormuth, V., Debrégeas, G. and Candelier, R. (2016). Rheotaxis of Larval Zebrafish: Behavioral Study of a Multi-Sensory Process. *Front Syst Neurosci* **10**,.

Pavlov, D. S. and Tyuryukov, S. N. (1993). The role of lateral-line organs and equilibrium in the behavior and orientation of the dace, Leuciscus leuciscus, in a turbulent flow. *J Ichthyol* **33**, 45–55.

Perrault, T. J., Stein, B. E. and Rowland, B. A. (2011). Non-stationarity in multisensory neurons in the superior colliculus. *Front Psychol* **2**,.

R Core Team (2022). R: A Language and Environment for Statistical Computing.

Richard, M. J. (1896). *Comptes rendus des séances de la Société de biologie et de ses filiales.* Paris,Masson [etc.].

Rieger, P. W. and Summerfelt, R. C. (1998). Microvideography of gas bladder inflation in larval walleye. *J Fish Biol* **53**, 93–99.

Riley, B. B. and Moorman, S. J. (2000). Development of utricular otoliths, but not saccular otoliths, is necessary for vestibular function and survival in zebrafish. *J Neurobiol* **43**, 329–337.

Santos, F., MacDonald, G., Rubel, E. W. and Raible, D. W. (2006). Lateral line hair cell maturation is a determinant of aminoglycoside susceptibility in zebrafish (Danio rerio). *Hear Res* **213**, 25–33.

Schoppik, D., Bianco, I. H., Prober, D. A., Douglass, A. D., Robson, D. N., Li, J. M. B., Greenwood, J. S. F., Soucy, E., Engert, F. and Schier, A. F. (2017). Gaze-stabilizing central vestibular neurons project asymmetrically to extraocular motoneuron pools. *Journal of Neuroscience* **37**, 11353–11365.

Schwartz, E. and Hasler, A. D. (1966). Perception of Surface Waves by the Blackstripe Topminnow, *Fundulus notatus*. *Journal of the Fisheries Research Board of Canada* **23**, 1331–1352.

Stewart, W. J., Cardenas, G. S. and McHenry, M. J. (2013). Zebrafish larvae evade predators by sensing water flow. *J Exp Biol* **216**, 388–98.

Stuart, K. R. and Drawbridge, M. (2012). The effect of photoperiod on larval culture performance of two marine finfish species. *Aquaculture* **360–361**, 54–57.

Suchocki, C. R. and Sepulveda-Villet, O. J. (2019). The role of phototaxis in the initial swim bladder inflation of larval yellow perch (Perca flavescens). *Int Aquat Res* **11**, 33–42.

Tait, J. S. (1960). The First Filling Of The Swim Bladder In Salmonoids. *Can J Zool* **38**, 179–187.

Thompson, A. W., Vanwalleghem, G. C., Heap, L. A. and Scott, E. K. (2016). Functional profiles of visual-, auditory-, and water flow-responsive neurons in the Zebrafish Tectum. *Current Biology* **26**, 743–754.

Trotter, A. J., Battaglene, S. C. and Pankhurst, P. M. (2003). Effects of photoperiod and light intensity on initial swim bladder inflation, growth and post-inflation viability in cultured striped trumpeter (Latris lineata) larvae. *Aquaculture* **224**, 141–158.

Tsukamoto, Y. and Yoshino, S. (1957). A Study of the Lateral-line System in Fish II. On the Relation between the Function of the Lateral-line Organ and the Habits of Fish. *Japanese Journal of Ichthyology* **6**, 131–135.

v. Ledebur, J. F. and Wunder, W. (1937). Beiträge zur Physiologie der Schwimmblase der Fische. *Zeitschrift für vergleichende Physiologie 1937 25:2* **25**, 149–155.

Venuto, A. and Erickson, T. (2021). Evaluating the Death and Recovery of Lateral Line Hair Cells Following Repeated Neomycin Treatments. *Life 2021, Vol. 11, Page 1180* **11**, 1180.

Venuto, A., Smith, C. P., Cameron-Pack, M. and Erickson, T. (2022). Alone in a crowd: effect of a nonfunctional lateral line on expression of the social hormone parathyroid hormone 2. *Biol Open* **11**,.

Villamizar, N., García-Alcazar, A. and Sánchez-Vázquez, F. J. (2009). Effect of light spectrum and photoperiod on the growth, development and survival of European sea bass (Dicentrarchus labrax) larvae. *Aquaculture* **292**, 80–86.

von Ledebur, J. Frhr. (1928). Beiträge zur Physiologie der Schwimmblase der Fische. *Z Vgl Physiol* **8**, 445–460.

Westerfield, M. (2000). *The zebrafish book. A guide for the laboratory use of zebrafish (Danio rerio).* 4th ed. Eugene OR: University of Oregon.

715 **Figures**

716

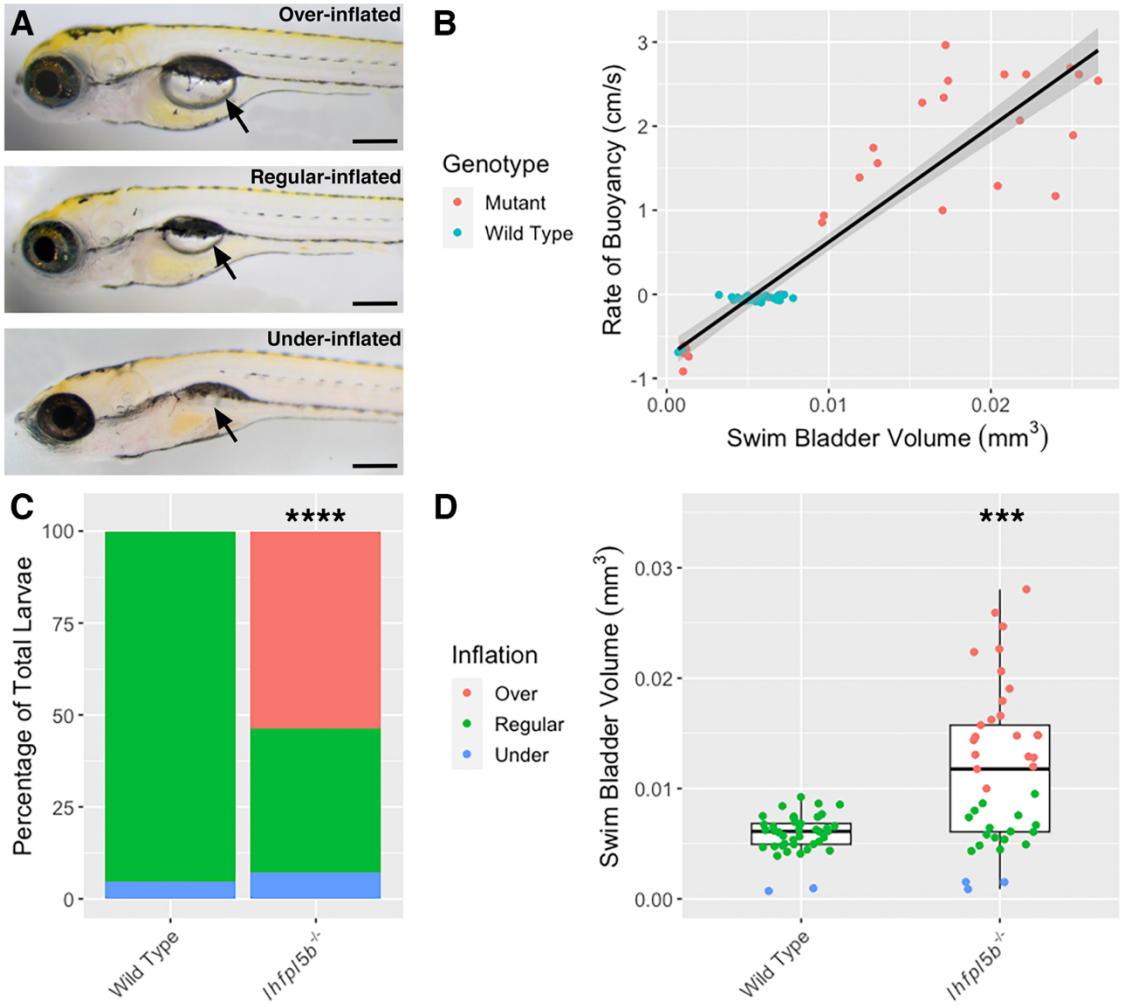

717

718 **Figure 1**. Hyperinflation of the swim bladder in lateral line mutants (*lhfpl5b*$^{-/-}$). A) Representative
719 examples of over-, regular, and under-inflated swim bladders (arrows) in larval zebrafish at 6 dpf
720 (top: *lhfpl5b*$^{-/-}$, others are wild type). B) Correlation between buoyancy and swim bladder volume.
721 Line of best fit applied through the combination of mutant and wild type data (linear model, R-
722 squared = 0.8574). C) Percentage of larvae that exhibit over-, regular, and under-inflation of the
723 swim bladder, as defined by positive, neutral, and negative buoyancy. A Chi-Squared Test was
724 used to determine significance. D) Swim bladder volume (mm^3) in wild type and *lhfpl5b* mutant
725 larvae at 6 dpf. A Welch's t-test was used to determine significance. *** = $p < 0.001$, **** = $p <$
726 0.0001. Scale bar = 0.2 mm.

727

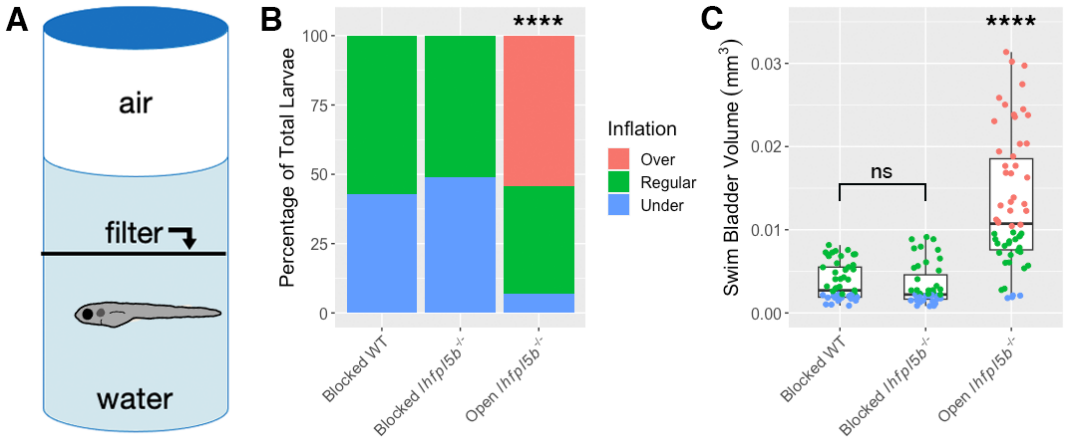

Figure 2: Blocking access to the surface eliminates the hyperinflation phenotype in lateral line mutants (*lhfpl5b*$^{-/-}$). A) Diagram of experimental set up with a filter blocking access to the surface. B) Percentage of larvae that exhibit over-, regular, and under-inflation of the swim bladder at 6 dpf. A Chi-Squared Test was used to determine significance. C) Swim bladder volume (mm^3) of larvae at 6 dpf. A One-Way ANOVA was used to determine significance. **** = $p < 0.0001$, , **** = $p < 0.0001$, ns = not significant. Full ANOVA table in supplemental tables.

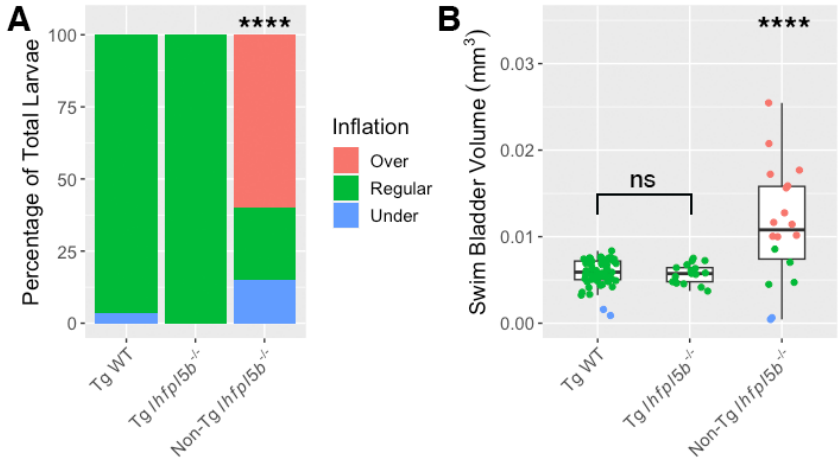

Figure 3: Rescue of lateral line mutants (*lhfpl5b*$^{-/-}$) with the *Tg(myo6b:EGFP-lhfpl5a)vo23* transgene. A) Percentage of larvae that exhibit swim bladder under, regular, and over-inflation at 6 dpf. A Chi-Squared Test was used to determine significance. B) Swim bladder volume (mm^3) of larvae at 6 dpf. A One-Way ANOVA was used to determine significance. **** = $p < 0.0001$, ns = not significant. Full ANOVA table in supplemental tables.

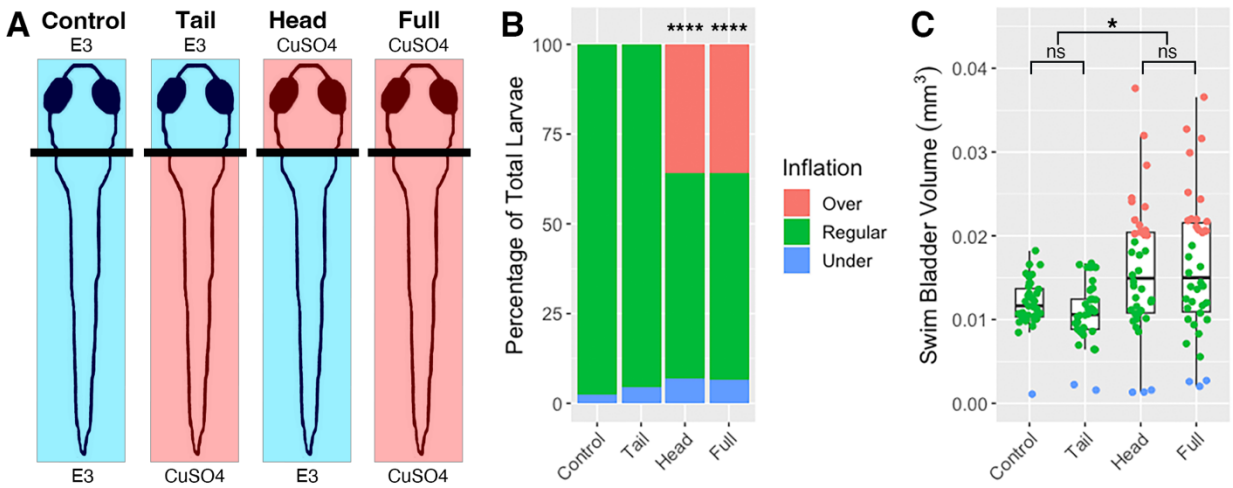

Figure 4: Head-specific ablations of the lateral line recapitulates the *lhfpl5b* mutant hyperinflation phenotype. A) Diagram of experiment. B) Percentage of larvae that exhibit swim bladder under, regular, and over-inflation at 5 dpf. A Chi-Squared Test was used to determine significance. C) Swim bladder volume (mm^3) of larvae at 5 dpf. A One-Way ANOVA was used to determine significance. * = $p < 0.05$, , **** = $p < 0.0001$, ns = not significant. Full ANOVA table in supplemental tables. Images of live larvae following treatment in Supplemental Figure 3.

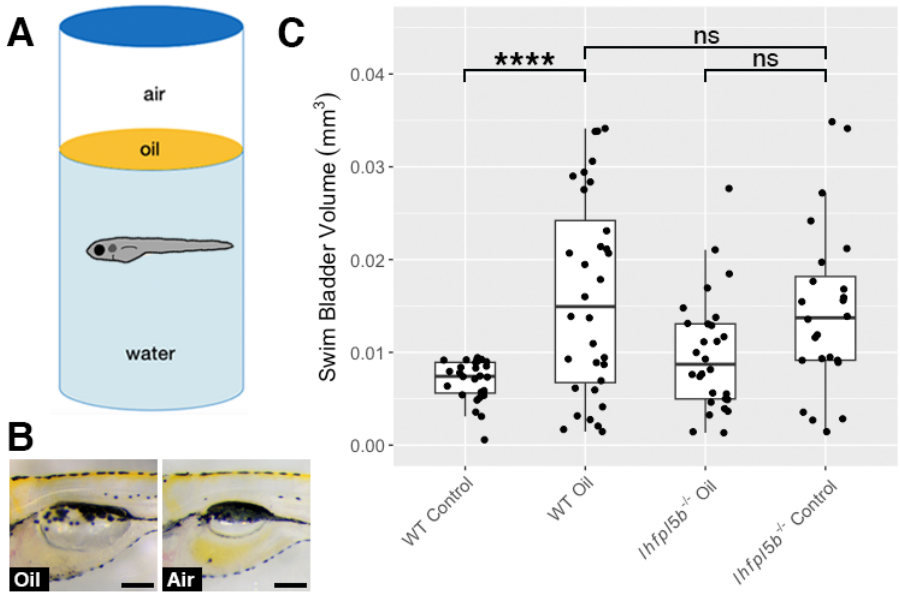

Figure 5: Decreasing interfacial surface tension with mineral oil results in over-filling of the swim bladder. A) Diagram of experiment with 2 mm layer of oil on surface. B) Images of swim bladder phenotypes resulting from surface oil and surface air exposure in wild type larvae at 6 dpf. C) Swim bladder volume (mm^3) at 6 dpf. A One-Way ANOVA was used to determine significance. * = $p < 0.05$, ns = not significant. Scale bar = 0.1 mm. Full ANOVA table in supplemental tables.

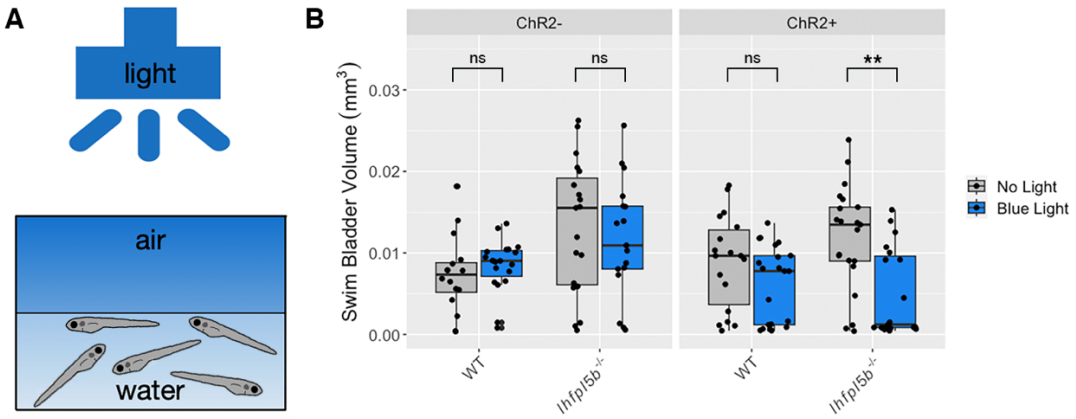

Figure 6: Optogenetic activation of lateral line hair cells with Channelrhodopsin-2 (ChR2) in wild type and *lhfpl5b* mutant larval zebrafish. A) Diagram of experiment with blue light stimuli delivered for 25 milliseconds at 1 second intervals. Treatments were started at 4 dpf and swim bladder volume was assessed at 6 dpf. B) Swim bladder volume (mm^3) of larvae at 6 dpf, n = 16-21 per condition. One-Way ANOVA was used to determine significance. ** = $p < 0.001$, ns = not significant. Full ANOVA table in supplemental tables.

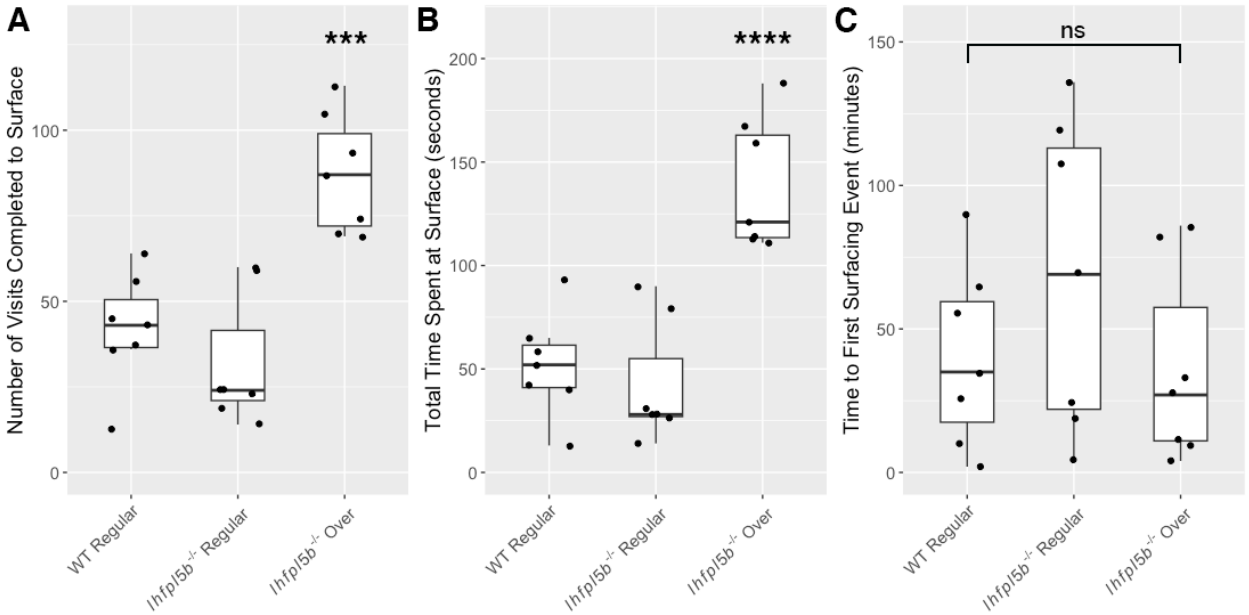

Figure 7: Quantification of the surfacing behaviors of wild type and *lhfpl5b* mutant zebrafish larvae during initial swim bladder inflation. A) Total number of individual visits taken by larval fish to the air-water interface on 4 dpf for 12 hours (9 AM – 9 PM). B) Total amount of time larval fish spend at the surface for all visits combined on 4 dpf. C) Time to first surface visit after access was allowed. A One-Way ANOVA was used to determine significance. *** = $p < 0.001$, ns = not significant.

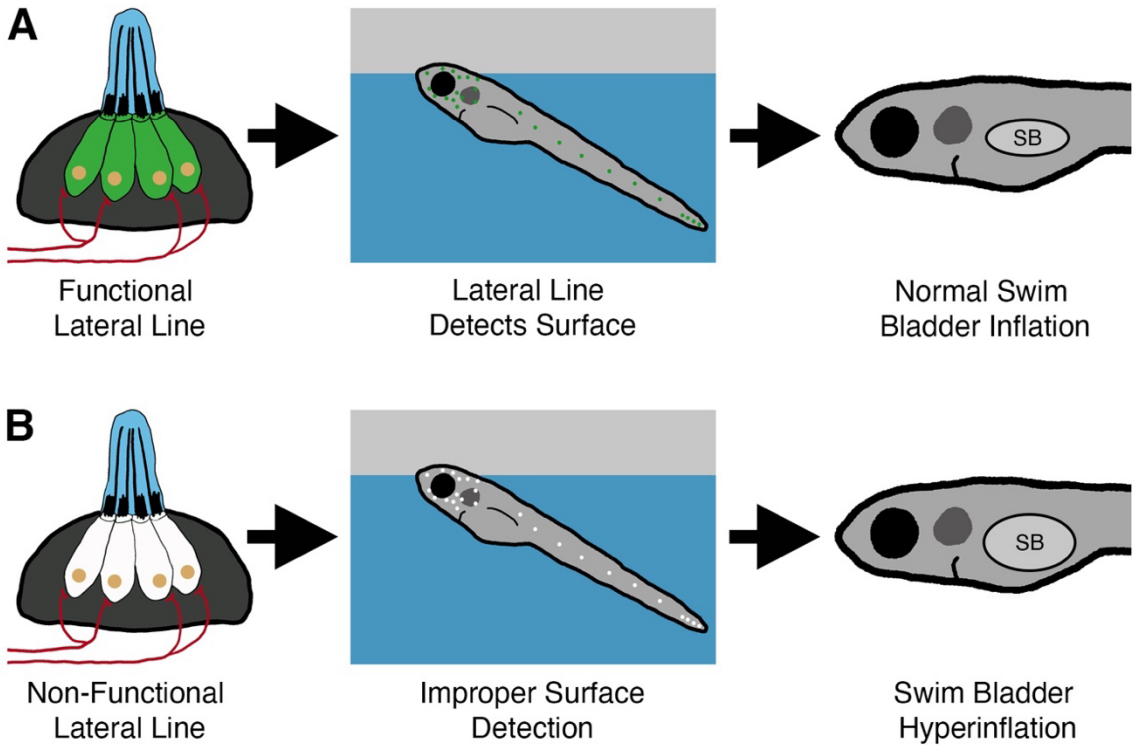

774
775 **Figure 8.** Summary of the surfacing behavior of wild type and lateral line-deficient zebrafish
776 larvae. A) Wild type larvae use their lateral line hair cells (in green) to mediate interactions with
777 the air-water interface during surfacing. As a result of accurate surface detection, larvae take in an
778 appropriate volume of air for swim bladder (SB) inflation and achieve neutral buoyancy. B) Larvae
779 with a genetic loss of lateral line function (hair cells in white) misinterpret the air-water interface,
780 leading to increased interactions with the surface. Consequently, lateral line mutants *(lhfpl5b*$^{-/-}$*)*
781 take in an excess volume of air, resulting in hyperinflation of the swim bladder for approximately
782 half of mutant larvae. Selective chemical ablations of the head neuromasts produce similar results,
783 implicating the anterior lateral line as the primary sensory organ for interactions with the air-water
784 interface during the surfacing behavior.
785

786 **Supplemental Figures**

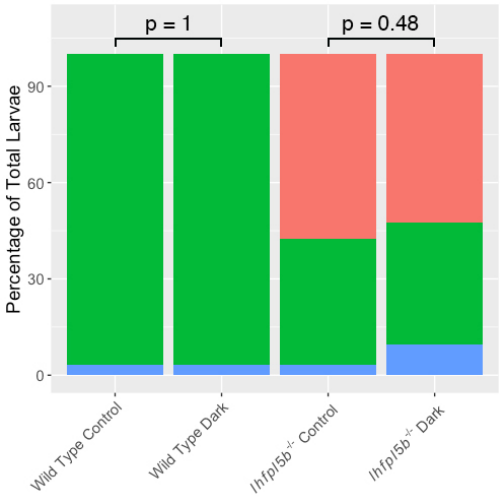

787
788 **Supplemental Figure 1.** Buoyancy status of larvae raised in total darkness. Percentage of larvae
789 that exhibit swim bladder under, regular, and over-inflation raised in either a 14:10 light/dark
790 cycle (Control) or total darkness (0:24 light/dark cycle). A Chi-Squared Test was used to assess
791 significance. Both Wild Type Control and Wild Type Dark over-inflation proportions: M = 0.0%,
792 SD = 0.0%, n = 32. *lhfpl5b*$^{-/-}$ Control over-inflation proportion: M = 57.5%, SD = 6.6%, n = 30.
793 *lhfpl5b*$^{-/-}$ Dark over-inflation proportion: M = 52.4%, SD = 4.1%, n = 30.
794

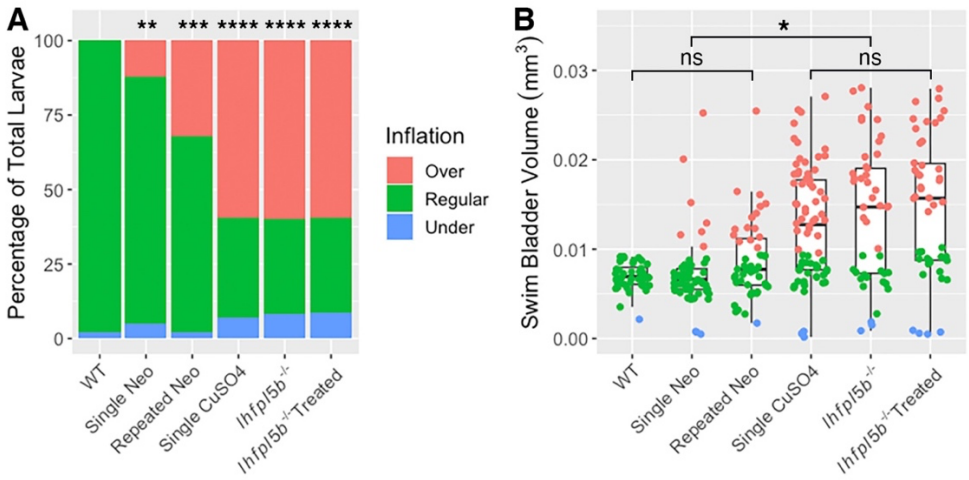

Supplemental Figure 2. Chemical ablations of lateral line hair cells phenocopies the hyperinflation phenotype of *lhfpl5b* mutants. A) Percentage of larvae treated with either neomycin or CuSO4 that exhibit swim bladder under, regular, and over-inflation. A Chi-Squared Test was used to assess significance. B) Swim bladder volume (mm^3) in 5 dpf larvae treated with either neomycin or CuSO4. A One-Way ANOVA was used to determine significance. **** = $p < 0.0001$, *** = $p < 0.001$, ** = $p < 0.01$, * = $p < 0.05$, ns = not significant. A full ANOVA table can be found in the supplemental tables.

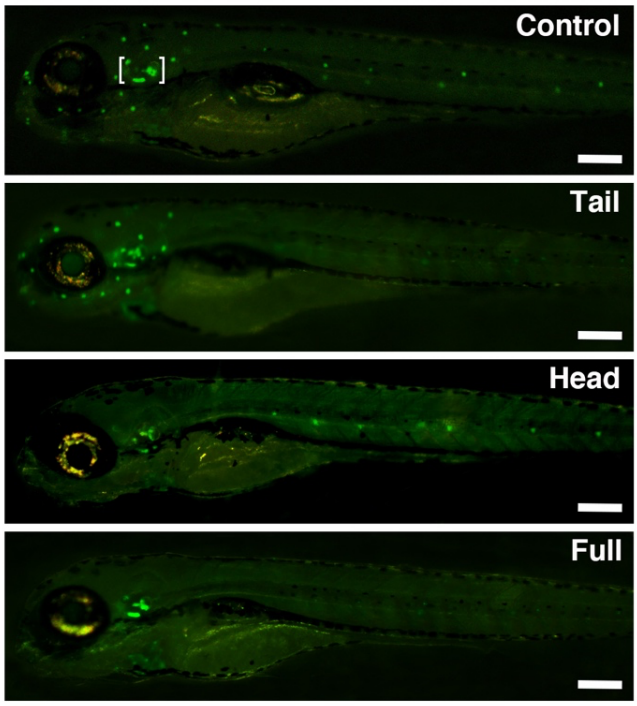

Supplemental Figure 3. Head and trunk-specific lateral line ablations with CuSO4. Representative images of live *Tg(myo6b:EGFP-PA)vo68* transgenics at 4 dpf, two hours after CuSO4 treatment. This transgene labels hair cells of the lateral line and inner ear (indicated by white brackets on the Control image). CuSO4 treatment ablates lateral line hair cells only, leaving inner ear hair cells intact.

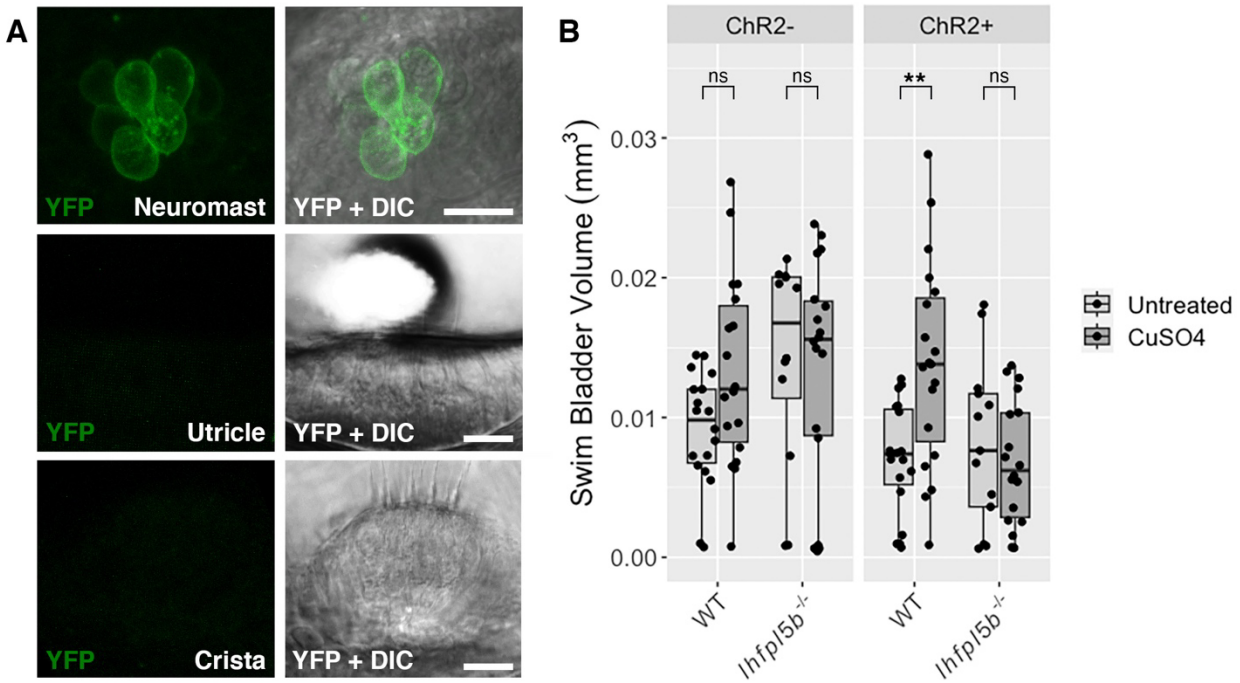

Supplemental Figure 4: A) Representative images of Channelrhodopsin-2 (ChR2) expression in neuromast, utricle, and crista hair cells of *Tg(lhfpl5b2028:ChR2-EYFP-PA)* transgenics at 2 dpf. ChR2-YFP expression is detectable only in the lateral line neuromasts, indicating specificity of the *lhfpl5b* regulatory region used to drive ChR2 expression. First panel is YFP only (false-colored green) and the second panel is a merge of YFP and DIC. Scale bars = 10 uM. B) Swim bladder volume (mm^3) of 6 dpf wild type and *lhfpl5b*$^{-/-}$ larvae, with and without the *ChR2* transgene. Groups of larvae were also treated with CuSO4 to ablate lateral line hair cells. All larvae were stimulated with blue light. The impacts of blue light stimulation on wild type ChR2 transgenics is abolished by chemical ablation of lateral line hair cells. As expected, *lhfpl5b* mutants are unaffected by CuSO4 treatment. A One-Way ANOVA was used to determine significance. ** = $p < 0.00724$, ns = not significant. A full ANOVA table can be found in the supplemental tables.